

UC Irvine

UC Irvine Previously Published Works

Title

A human-driven decline in global burned area.

Permalink

<https://escholarship.org/uc/item/6b42q71s>

Journal

Science (New York, N.Y.), 356(6345)

ISSN

0036-8075

Authors

Andela, N
Morton, DC
Giglio, L
[et al.](#)

Publication Date

2017-06-01

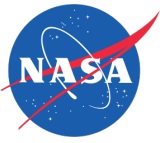
DOI

10.1126/science.aal4108

Copyright Information

This work is made available under the terms of a Creative Commons Attribution License, available at <https://creativecommons.org/licenses/by/4.0/>

Peer reviewed



Published in final edited form as:

Science. 2017 June 30; 356(6345): 1356–1362. doi:10.1126/science.aal4108.

A human-driven decline in global burned area

N. Andela^{1,2}, D.C. Morton¹, L. Giglio³, Y. Chen², G.R. van der Werf⁴, P.S. Kasibhatla⁵, R. S. DeFries⁶, G. J. Collatz¹, S. Hantson⁷, S. Kloster⁸, D. Bachelet⁹, M. Forrest¹⁰, G. Lasslop⁸, F. Li¹¹, S. Mangeon¹², J. R. Melton¹³, C. Yue¹⁴, and J.T. Randerson²

¹Biospheric Sciences Laboratory, NASA Goddard Space Flight Center, Greenbelt, MD 20771, USA

²Department of Earth System Science, University of California, Irvine, CA 92697, USA

³Department of Geographical Sciences, University of Maryland, College Park, MD 20742, USA

⁴Faculty of Earth and Life Sciences, Vrije Universiteit Amsterdam, Amsterdam, the Netherlands

⁵Nicholas School of the Environment, Duke University, Durham, NC 27708, USA

⁶Department of Ecology, Evolution, and Environmental Biology, Columbia University, New York, NY 10027, USA

⁷Karlsruhe Institute of Technology, Institute of Meteorology and Climate research, Atmospheric

Environmental Research, 82467 Garmisch-Partenkirchen, Germany

⁸Max Planck Institute for Meteorology, Bundesstraße 53, 20164 Hamburg, Germany

⁹Biological and Ecological Engineering, Oregon State University, Corvallis, OR 97331, USA

¹⁰Senckenberg Biodiversity and Climate Research Institute (BiK-F), Senckenberganlage 25, 60325 Frankfurt am Main, Germany

¹¹International Center for Climate and Environmental Sciences, Institute of Atmospheric Physics, Chinese Academy of Sciences, Beijing, China

¹²Department of Physics, Imperial College London, London, UK

¹³Climate Research Division, Environment Canada, Victoria, BC, V8W 2Y2, Canada

¹⁴Laboratoire des Sciences du Climat et de l'Environnement, LSCE/IPSL, CEA-CNRS-UVSQ, Université Paris-Saclay, 91198 Gif-sur-Yvette, France

Abstract

Fire is an essential Earth System process that alters ecosystem and atmospheric composition. Here we assessed long-term fire trends using multiple satellite datasets. We found that global burned area declined by $24.3 \pm 8.8\%$ over the past 18 years. The estimated decrease in burned area remained robust after adjusting for precipitation variability and was largest in savannas.

Agricultural expansion and intensification were primary drivers of declining fire activity. Fewer and smaller fires reduced aerosol concentrations, modified vegetation structure, and increased the magnitude of the terrestrial carbon sink. Fire models were unable to reproduce the pattern and magnitude of observed declines, suggesting they may overestimate fire emissions in future projections. Using economic and demographic variables, we developed a conceptual model for predicting fire in human-dominated landscapes.

Introduction

Fires play an integral role in shaping ecosystem properties (1) and have widespread impacts on climate, biogeochemical cycles and human health (2–4). Frequent fires are essential for maintaining savanna ecosystems (5), while more episodic events in temperate and boreal forests create a mosaic of habitats in different stages of post-fire succession (6). Introduction or exclusion of fire from the landscape may lead to rapid shifts in vegetation structure and

composition (5), carbon stocks (7), and biodiversity (8). Globally, fire emissions are responsible for 5 to 8% of the 3.3 million annual premature deaths from poor air quality, and fire is the primary cause of elevated mortality from air pollution across much of the tropics (3). Fires affect global climate through changes in vegetation and soil carbon (7), surface albedo (9), and atmospheric concentrations of aerosols and greenhouse gases (10). Climate feedbacks on fire activity are complex and vary by biome and level of fire suppression (11). Given projected increases in fire risk from climate change (12), fire management will be increasingly important for maintaining ecosystem function, air quality, and other services that influence human well-being (13).

Climate is a dominant control on fire activity, regulating vegetation productivity and fuel moisture. Over short time scales, rainfall during the dry season suppresses fire activity, while over longer time scales, fuel build up during wet years in more arid ecosystems can increase burned area in subsequent years (11). The redistribution of precipitation in response to El Niño Southern Oscillation (ENSO) and other climate modes therefore has a large and sometimes contrasting effect on the inter-annual and decadal variability of biomass burning across continents (6, 14, 15). Oscillations in Pacific and Atlantic sea surface temperatures also influence trends in fire activity on longer time scales (6, 15). Climate change may increase fire risk in many regions (12, 16), based on projected warming and drying in forests and other biomes with sufficient fuel loads to support fire activity. Ultimately, the interactions among climate, vegetation, and ignition sources determine the spatial and temporal pattern of biomass burning (17).

In addition to natural processes, humans have shaped patterns of global burning for millennia (4) and human activity is now the primary source of ignitions in tropical forests, savannas, and agricultural regions (14, 18). Human influence on fire dynamics depends on population density (17), socio-economic development (19), landscape fragmentation (18), and land management (15), as people introduce or suppress fires (4) and manipulate the timing and fuel conditions of fires in human-dominated landscapes (11, 14). During the past two decades, human population increased by about 25%, or 1.5 billion (20), and agricultural production increased by more than 40% (21). Today, about 36% of the world's land surface is used for pasture or croplands (22), directly affecting the way fire is managed within these ecosystems. Earlier work has demonstrated that cropland expansion or deforestation rates are closely linked to regional fire trends (14, 15), and, for many regions, changing fire activity in recent decades extends a long-term transition from natural to human-dominated fire regimes (23–25). However, global implications of changing agricultural management and the mechanisms that regulate fires in human-dominated landscapes remain poorly understood. Even in areas dominated by human sources of ignition, variations in precipitation and other weather conditions may modulate year-to-year variations in ignition efficiency, fire spread rate, and fire size. The interactions among fire weather, fuels, and ignition therefore make it challenging to separate climate and human controls on fire dynamics at regional and global scales. Nevertheless, this separation is necessary to build and improve predictive fire models.

Satellite-derived burned area data provide a consistent global perspective on changing patterns of fire activity. Here, we analyzed long-term trends in burned area from 1998–2015

using the Global Fire Emissions Database version 4 product that includes small fires (26, 27). We conducted several analyses to assess the drivers and implications of long-term trends in burned area (28). First, we estimated the influence of precipitation on burned area variability and trends in each 0.25° grid cell using a statistical model to separate climate and human contributions to fire trends (Fig. S1). Second, we separated burned area into contributions from the number and size of individual large fires using 500m resolution burned area data from NASA's Moderate Resolution Imaging Spectroradiometer (MODIS) sensors (29) during 2003–2015 (Fig. S2). Third, we compared observed trends with prognostic fire model estimates from the Fire Model Intercomparison Project (FireMIP), with the aim of understanding limits to fire prediction. Fourth, we examined spatial and temporal relationships between burned area and socio-economic data to investigate patterns of human influence on fire activity. Based on these data, we developed a conceptual model of fire use that considers the roles of land management and socioeconomic development. Finally, we assessed the impact of the observed decreasing burned area trend on ecosystem structure, the magnitude of the terrestrial carbon sink, and atmospheric composition in biomass burning regions. Together, these results underscore the pervasive influence of human activity on global burned area, including the potential for further declines in savanna fires from ongoing agricultural development across the tropics.

Trends in burned area

Global burned area declined by nearly one quarter between 1998 and 2015 ($-24.3 \pm 8.8\%$, or $-1.35 \pm 0.49\% \text{ yr}^{-1}$). Large decreases occurred in tropical savannas of South America and Africa and grasslands across the Asian steppe (Fig. 1). Globally, decreases were concentrated in regions with low and intermediate levels of tree cover, while an increasing trend was observed in closed-canopy forests. Declining trends were robust when assessed using different burned area datasets and time intervals (Table 1 and Fig. S3). GFED4s and MODIS 500m burned area data showed a similar decline during 2003–2015 ($-1.28 \pm 0.96\% \text{ yr}^{-1}$ and $-1.15 \pm 1.21\% \text{ yr}^{-1}$, respectively), and satellite-based active fire detections from MODIS provided an independent confirmation of the patterns of decreasing global fire activity (Fig. S4). Regional increases in burned area were also observed, but areas with a significant decline ($p < 0.05$) in burned area outnumbered areas with a significant increase in burned area for all continents except Eurasia (Fig. S5). For tropical savannas and grasslands, declines outnumbered increases by 3:1. Within individual continents, strong contrasting trends were observed between northern and southern Africa, and between Central America and temperate North America (Table S1).

Rainfall patterns explained much of the inter-annual variability in burned area but little of the long-term decline (Table 1, Fig. 2a). Building on previous work (15), we developed a linear model to adjust for the influence of precipitation variability on burned area (28, Fig. S6). Long-term trends were more significant after reducing precipitation-driven variability. For example, the global decline in burned area of $-1.15 \pm 1.21\% \text{ yr}^{-1}$ (2003–2015, $p < 0.1$) in the 500m MODIS time series strengthened to $-1.23 \pm 0.44\% \text{ yr}^{-1}$ ($p < 0.01$) after adjusting for precipitation (Table 1). Regionally, precipitation adjusted burned area time series showed significant declines in Central America, northern hemisphere South America, Europe, northern hemisphere Africa, and Central Asia (Table S1).

A decrease in the number of fires explained most of the global decline in burned area, with a smaller contribution from decreasing mean fire size (Fig. 2). The relative contributions from fire number and fire size to observed trends varied considerably among regions (Table 1, Fig. S7). In northern Africa, the number and mean size of fires contributed nearly equally to the net decline in burned area. In contrast, a decrease in the number of fires was the primary factor causing a decline in burned area in South America, Central America and Central Asia (Table S1). Regional and inter-annual variability in the size distribution of individual fires provided new information about the combined influence of climate, landscape fragmentation, and management on burned area; this information is essential for improving representation of fire in Earth System models.

Current global fire models were unable to predict the magnitude or spatial pattern of the observed decline in global burned area (Fig. 3, S8–S10). During 1997–2013, FireMIP models ($n=9$) predicted a mean trend in global burned area of $-0.13 \pm 0.56\% \text{ yr}^{-1}$, compared to the observed trend of $-1.09 \pm 0.61\% \text{ yr}^{-1}$ for this interval (28, Table 1 and S2). Focusing on the three models that account for human contributions to the number and size of fires (Table S3), two models predicted a small decline in global burned area, but often poorly simulated the spatial structure of trends across different continents (Fig. 3 and S8). Despite including land use and population as input variables, several models predicted increasing burned area (28, Table S4), consistent with global trends in fire weather (16). These model-data differences highlight the pervasive influence of human activity in reducing burning despite growing climate-driven fire risk.

Humans as a driver of the long-term trend

Population, cropland area, and livestock density were important factors constraining landscape patterns of burning, yet the sign and magnitude of the spatial correlation coefficient between these variables and burned area varied across biomes and along gradients of tree cover (Fig. 4). All three indicators had negative spatial correlations with burned area in savannas and grasslands. Although these three variables had similar global structure, we found that the distribution of agricultural activity clearly modified burned area beyond population alone. For example, widespread agricultural waste burning in large parts of Asia generated a strong positive correlation between cropland and burned area. Similarly, livestock density and burned area were negatively correlated in the Brazilian Cerrado, as livestock may directly suppress fire activity by reducing fuel loads or altering fire management decisions. In tropical forests, population density and cropland were positively correlated with the spatial pattern of burned area, as humans have introduced fires for deforestation and agricultural management (7, 27). In boreal forests, we found a stronger positive relationship between population and burned area in Eurasia than North America, consistent with past work documenting high levels of human-driven fire activity in Russia (30). Trends in agricultural production and fire activity were also consistent at the national scale. The largest relative declines in GFED4s burned area occurred in countries with the largest increases in agricultural extent and production value (Fig. S11).

We developed a conceptual model of changes in burned area with increasing development based on spatial patterns of burned area, land use, population density, and gross domestic

product (GDP) data (Fig. 5). Our analysis showed that the evolution of human-dominated fire regimes follows predictable patterns, with the transition from natural to managed landscapes in forest and savanna regions generating markedly different burned area trajectories (28, Fig. S12 and S13). For humid tropical forests, frequent fires for deforestation and agricultural management yielded a sharp rise in fire activity with the expansion of settled land uses, providing quantitative evidence for rapid ecosystem transformation during early land use transitions described in previous work (31, 32). However, in semi-arid savannas and grasslands, the transition from natural landscapes with common land ownership to agriculture on private lands generated a non-linear decrease in fire activity, even in areas without large-scale land cover conversion. The reorganization of land cover and fire use on the landscape also altered the contributions from different fire types to total burned area (Fig. 5). For both forested and savanna regions, the most rapid changes in both land cover and total burned area occurred for transitions at very low levels of per capita GDP ($< \$5,000 \text{ km}^{-2} \text{ yr}^{-1}$, Fig. S12 and S13).

With an expanding human presence on the landscape, increasing investment in agricultural areas reduced fire activity in both savannas and forests (Fig. 5). In highly capitalized regions, burned area was considerably lower, likely as a consequence of both mechanized (fire-free) management and fire suppression to protect high-value crops, livestock, homes, infrastructure, and air quality (13, Fig. 4, 5 and S11). Livelihoods change drastically along this trajectory of fire use, as does the perception of fire and smoke (23). Regulation to improve air quality has significantly reduced cropland burning in the western US (33). In contrast, fire activity increased in some densely populated agricultural regions of India and China (Fig. 1 and 4), suggesting that without investments in air quality management, agricultural intensification may increase fire activity in regions where crop residue burning is the dominant fire type. Agricultural expansion and intensification are likely to continue in coming decades (21), with largest changes expected in the tropics, as development shifts vast areas of common land or extensive land uses towards more capital intensive agricultural production for regional or global markets (21, 32). These changes in land use suggest that observed declines in burned area may continue or even accelerate in coming decades.

Successful prediction of fire trends on decadal timescales requires a mechanistic description of fire use during the different phases of development shown in Fig. 5. Considering the observational constraints described here, we identified three primary reasons why the FireMIP models were unable to reproduce the observed decline in global burned area. First, all FireMIP models underestimated the magnitude of burned area declines in areas with moderate and high densities of population and per capita GDP (Fig. S14), suggesting the models were not sensitive enough to the influence of economic development on fire activity. Second, while many of the FireMIP models included pasture area as a variable describing human modification of land cover, burning in pasture areas was often treated the same as grasslands (Table S3), and in many tropical countries, most land areas available for grazing had been converted to pasture by the 1970s. The relative saturation of changing pasture area during the past two decades contrasted sharply with very large increases in livestock density (Fig. S15), highlighting the importance of better integrating drivers of land use intensification within prognostic models. Third, fire models overestimated burned area in semi-arid tropical ecosystems and underestimated burned area in mesic and humid tropical

ecosystems (Fig. S14). This bias in the spatial distribution of burned area may have weakened the models' overall sensitivity to human development drivers, since population and wealth changes were more pronounced in areas with higher levels of rainfall. While the spatial pattern of burned area has been widely used as a target for fire model development in past work (34, Fig. S9), our analysis highlights the importance of using trend and fire size observations to constrain scenarios of future fire activity (Fig. S10 and Table S5).

Implications of declining global fire activity

The observed large-scale decline of burned area in the world's grasslands, savannas, and tropical land use frontiers had broad consequences for vegetation dynamics, carbon cycling, air quality, and biodiversity. Fires play an important role in the regulating the competition between herbaceous and woody vegetation (5). In grid cells where burned area was equal to or exceeded $10\% \text{ yr}^{-1}$, we found that the spatial pattern of trends in both dry season enhanced vegetation index (EVI) and vegetation optical depth (VOD) were negatively correlated with trends in burned area, consistent with woody encroachment in areas with declining burned area (28, Table S6, Fig. S16). However, further analysis of higher resolution satellite imagery is necessary to quantify the magnitude of encroachment in areas with significant fire trends as well as other mechanisms that may influence vegetation indices.

Less frequent burning also allowed biomass, litter and soil organic matter stocks to accumulate, contributing to a 0.2 Pg yr^{-1} carbon sink by 2015 in tropical and temperate savannas and grasslands (28, Fig. S17, $40^{\circ}\text{N} - 40^{\circ}\text{S}$). Placing this estimate in the context of the global carbon cycle, declining savanna and grassland fires accounted for about 7% of the contemporary global net land flux (35) and were likely an important driver of the large and variable terrestrial carbon sink previously reported in semi-arid ecosystems (36). Our estimate of the fire contribution to the terrestrial carbon sink is likely conservative because the biogeochemical model we used did not account for burned area changes prior to 2001, declining emissions in deforestation zones, or woody encroachment in regions with declining fire frequency (27, 28).

Analysis of satellite observations of aerosol and carbon monoxide concentrations provided independent evidence of declining fire emissions. Declining fire emissions lowered aerosol concentrations in the major tropical biomass burning regions during the fire season (Fig. S4b), leading to improved air quality and regional changes in radiative forcing and atmospheric composition. Although atmospheric transport distributes fire emissions across large areas, we identified a strong local effect of declining burned area on aerosol absorption optical depth in frequently burning grid cells ($r = 0.26$, $p < 0.01$, Table S6). Similarly, declining fire activity also lowered regional carbon monoxide concentrations ($r = 0.11$, $p < 0.01$, Fig S4c), suggesting that decreasing biomass burning emissions may have partly offset other drivers of increasing atmospheric methane (37).

Declining fire frequency supports climate mitigation efforts but may run counter to conservation objectives in fire-dependent ecosystems. Frequent fires are a key aspect of many ancient grassland ecosystems that support a range of endemic species (38) and a large

portion of the worlds remaining wild large mammals (39). The magnitude of habitat and biodiversity losses from declining burned area in savanna and grassland ecosystems may equal or exceed other human impacts in the tropics (Fig. 1), but these impacts have been largely neglected by the international community (40). Challenges for conserving savanna ecosystems abound; tradeoffs among conservation, climate mitigation, human health, and agricultural production will ultimately determine the balance of fire activity in savannas and grasslands (Figs. 4, 5, S4, S16, and S17).

The strong and sustained burned area declines in grasslands and savannas documented here represent a first-order impact on the Earth system, with consequences for ecosystems and climate that may be comparable with other large-scale drivers of global change. A shift toward more capital-intensive agriculture has led to fewer and smaller fires, driven by population increases, socio-economic development, and demand for agricultural products from regional and global markets. Together, these factors influence fire use in predictable ways, with a strong inverse relationship between burned area and economic development (Fig. 5). The pervasive influence of human activity on burned area was not captured by state-of-the-art fire models; improving these models in the future may require a more sophisticated representation of land use intensification and its influence on fire dynamics. Despite potential increasing fire risk from climate change (12, 16), ongoing socio-economic development will likely sustain observed declines in fire in savanna and grassland ecosystems in coming decades, altering vegetation structure and biodiversity. Fire is one of the oldest tools for human landscape management, yet the use of fire is rapidly changing in response to the expansion of global agriculture. Achieving a balance between conservation of fire-dependent ecosystems and increasing agricultural production to support growing populations will require careful management of fire activity in human-dominated landscapes.

Supplementary Material

Refer to Web version on PubMed Central for supplementary material.

Acknowledgments

N.A, Y.C. and J.R. received funding from the Gordon and Betty Moore Foundation (grant GBMF3269), D.M. was supported by NASA's Interdisciplinary Science and Carbon Monitoring System Programs, G.v.d.W. was supported by the Netherlands Organisation for Scientific Research (NWO), S.H. by the EU FP7 projects BACCHUS (grant 603445) and LUC4C (grant 603542), L.F. by the National Science Foundation of China (grant 41475099) and C.Y. by the ESA firecci project. We would like to thank M. N. Deeter for his helpful suggestions on MOPITT CO analysis. The authors declare that they have no competing interests. Data used in this study are available at www.globalfiredata.org<http://reverb.echo.nasa.gov>www.gpcp.umd.eduwww.faostat3.fao.org<http://web.omi.gov/sci/landscan> and are described in more detail in the Supplementary Materials. FireMIP model simulation output is archived with the supporting information, and full datasets are available on request.

References and Notes

1. Bond WJ, Woodward FI, Midgley GF. The global distribution of ecosystems in a world without fire. *New Phytol.* 2005; 165:525–537. [PubMed: 15720663]
2. Crutzen PJ, Andreae M. Biomass burning in the tropics: Impact on atmospheric chemistry and biogeochemical cycles. *Science.* 1990; 250:1669–1678. [PubMed: 17734705]

3. Lelieveld J, Evans JS, Fnais M, Giannadaki D, Pozzer A. The contribution of outdoor air pollution sources to premature mortality on a global scale. *Nature*. 2015; 525:367–371. [PubMed: 26381985]
4. Bowman DMJS, et al. Fire in the Earth system. *Science*. 2009; 324:481–484. [PubMed: 19390038]
5. Scholes RJ, Archer SR. Tree-grass interactions in savannas. *Annu. Rev. Ecol. Syst.* 1997; 28:517–544.
6. Swetnam TW, Betancourt JL. Fire-Southern Oscillation relations in the southwestern United States. *Science*. 1990; 249:1017–1020. [PubMed: 17789609]
7. Page SE, et al. The amount of carbon released from peat and forest fires in Indonesia during 1997. *Nature*. 2002; 420:61–65. [PubMed: 12422213]
8. Cochrane MA, Schulze MD. Fire as a recurrent event in tropical forests of the eastern Amazon: effects on forest structure, biomass, and species composition. *Biotropica*. 1999; 31:2–16.
9. Randerson JT, et al. The impact of boreal forest fire on climate warming. *Science*. 2006; 314:1130–1132. [PubMed: 17110574]
10. Ward DS, et al. The changing radiative forcing of fires: global model estimates for past, present and future. *Atmos. Chem. Phys.* 2012; 12:10857–10886.
11. Archibald S, Nickless A, Govender N, Scholes RJ, Lehsten V. Climate and the inter-annual variability of fire in southern Africa: a meta-analysis using long-term field data and satellite-derived burnt area data. *Glob. Ecol. Biogeogr.* 2010; 19:794–809.
12. Pechony O, Shindell DT. Driving forces of global wildfires over the past millennium and the forthcoming century. *Proc. Natl. Acad. Sci. U. S. A.* 2010; 107:19167–19170. [PubMed: 20974914]
13. Moritz MA, et al. Learning to coexist with wildfire. *Nature*. 2014; 515:58–66. [PubMed: 25373675]
14. Aragao L, et al. Interactions between rainfall, deforestation and fires during recent years in the Brazilian Amazonia. *Philos. Trans. R. Soc. B.* 2008; 363:1779–1785.
15. Andela N, van der Werf GR. Recent trends in African fires driven by cropland expansion and El Niño to La Niña transition. *Nat. Clim. Chang.* 2014; 4:791–795.
16. Jolly WM, et al. Climate-induced variations in global wildfire danger from 1979 to 2013. *Nat. Commun.* 2015; 6:7537. [PubMed: 26172867]
17. Bistinas I, Harrison SP, Prentice IC, Pereira JMC. Causal relationships versus emergent patterns in the global controls of fire frequency. *Biogeosciences*. 2014; 11:5087–5101.
18. Archibald S, Roy DP, van Wilgen BW, Scholes RJ. What limits fire? An examination of drivers of burnt area in Southern Africa. *Glob. Chang. Biol.* 2009; 15:613–630.
19. Chuvieco E, Justice CO. *Advances in Earth Observation of Global Change* Chuvieco E, Li J, Yang X, editors 2010 187199
20. United States Census Bureau. Historical estimates of world population (available at <http://www.census.gov>).
21. Alexandratos N, Bruinsma J. Food and Agriculture Organization, World agriculture towards 2030/2050: the 2012 revision. ESA Work. Pap. No. 12-03. 2012
22. Ramankutty N, Evan AT, Monfreda C, Foley JA. Farming the planet: 1. Geographic distribution of global agricultural lands in the year 2000. *Global Biogeochem. Cycles*. 2008; 22:1–16.
23. Pyne SJ. *Fire in America. A cultural history of wildland and rural fire* Princeton University Press; 1982
24. van Marle MJE, et al. Historic global biomass burning emissions based on merging satellite observations with proxies and fire models (1750–2015). *Geosci. Model Dev. Discuss.* 2017; doi: 10.5194/gmd-2017-32
25. Marlon JR, et al. Climate and human influences on global biomass burning over the past two millennia. *Nat. Geosci.* 2008; 1:697–702.
26. Randerson JT, Chen Y, van der Werf GR, Rogers BM, Morton DC. Global burned area and biomass burning emissions from small fires. *J. Geophys. Res.* 2012; 117:G04012.
27. van der Werf GR, et al. Global fire emissions estimates during 1997–2015. *Earth Syst. Sci. Data Discuss.* 2017; doi: 10.5194/essd-2016-62
28. Materials and methods are available as supplementary materials at the Science website.

29. Giglio L, Loboda T, Roy DP, Quayle B, Justice CO. An active-fire based burned area mapping algorithm for the MODIS sensor. *Remote Sens. Environ.* 2009; 113:408–420.
30. Mollicone D, Eva HD, Archard F. Human role in Russian wild fires. *Nature.* 2006; 440:436–437. [PubMed: 16554800]
31. Foley JA, et al. Global consequences of land use. *Science.* 2005; 309:570–4. [PubMed: 16040698]
32. Rudel TK, Defries R, Asner GP, Laurance WF. Changing drivers of deforestation and new opportunities for conservation. *Conserv. Biol.* 2009; 23:1396–1405. [PubMed: 20078640]
33. Lin H-W, et al. Management and climate contributions to satellite-derived active fire trends in the contiguous United States. *J. Geophys. Res. Biogeosciences.* 2014; 119:645–660.
34. Rabin SS, et al. The Fire Modeling Intercomparison Project (FireMIP), phase 1: experimental and analytical protocols with detailed model descriptions. *Geosci. Model Dev.* 2016; 10:1175–1197.
35. Le Quéré C, et al. Global carbon budget 2014. *Earth Syst. Sci. Data.* 2015; 7:47–85.
36. Ahlstrom A, et al. The dominant role of semi-arid ecosystems in the trend and variability of the land CO₂ sink. *Science.* 2015; 348:895–899. [PubMed: 25999504]
37. Rice AL, et al. Atmospheric methane isotopic record favors fossil sources flat in 1980s and 1990s with recent increase. *Proc. Natl. Acad. Sci.* 2016; 113:10791–10796. [PubMed: 27621453]
38. Bond WJ. Ancient grasslands at risk. *Science.* 2016; 351:120–122. [PubMed: 26744392]
39. Hempson GP, et al. A continent-wide assessment of the form and intensity of large mammal herbivory in Africa. *Science.* 2015; 350:1056–1061. [PubMed: 26612946]
40. Parr CL, Lehmann CER, Bond WJ, Hoffmann WA, Andersen AN. Tropical grassy biomes: Misunderstood, neglected, and under threat. *Trends Ecol. Evol.* 2014; 29:205–213. [PubMed: 24629721]
41. Pellegrini AFA. Nutrient limitation in tropical savannas across multiple scales and mechanisms. *Ecology.* 2016; 97:313–324. [PubMed: 27145607]
42. van der Werf GR, et al. Global fire emissions and the contribution of deforestation, savanna, forest, agricultural, and peat fires (1997–2009). *Atmos. Chem. Phys.* 2010; 10:11707–11735.
43. Giglio L, Randerson JT, van der Werf GR. Analysis of daily, monthly, and annual burned area using the fourth-generation global fire emissions database (GFED4). *J. Geophys. Res. Biogeosciences.* 2013; 118:317–328.
44. Wooster M, Roberts G, Perry GLW, Kaufman Y. Retrieval of biomass combustion rates and totals from fire radiative power observations: FRP derivation and calibration relationships between biomass consumption. *J. Geophys. Res.* 2005; 110:D24311.
45. Wessels KJ, et al. Can human-induced land degradation be distinguished from the effects of rainfall variability? A case study in South Africa. *J. Arid Environ.* 2007; 68:271–297.
46. Evans J, Geerken R. Discrimination between climate and human-induced dryland degradation. *J. Arid Environ.* 2004; 57:535–554.
47. Andela N, Liu YY, van Dijk AIJM, de Jeu RAM, McVicar TR. Global changes in dryland vegetation dynamics (1988–2008) assessed by satellite remote sensing: comparing a new passive microwave vegetation density record with reflective greenness data. *Biogeosciences.* 2013; 10:6657–6676.
48. Herrmann SM, Anyamba A, Tucker CJ. Recent trends in vegetation dynamics in the African Sahel and their relationship to climate. *Glob. Environ. Chang.* 2005; 15:394–404.
49. Tian F, Brandt M, Liu YY, Rasmussen K, Fensholt R. Mapping gains and losses in woody vegetation across global tropical drylands. *Glob. Chang. Biol.* 2016; 23:1748–1760. [PubMed: 27515022]
50. van der Werf GR, Randerson JT, Giglio L, Gobron N, Dolman AJ. Climate controls on the variability of fires in the tropics and subtropics. *Global Biogeochem. Cycles.* 2008; 22:1–13.
51. Chen Y, et al. Forecasting fire season severity in South America using sea surface temperature anomalies. *Science.* 2011; 334:787–791. [PubMed: 22076373]
52. Huffman GJ, et al. The TRMM Multisatellite Precipitation Analysis (TMPA): Quasi-Global, Multiyear, Combined-Sensor Precipitation Estimates at Fine Scales. *J. Hydrometeorol.* 2007; 8:38–55.

53. Adler RF, et al. The Version-2 Global Precipitation Climatology Project (GPCP) Monthly Precipitation Analysis (1979–Present). *J. Hydrometeorol.* 2003; 4:1147–1167.
54. Huffman GJ, Adler RF, Bolvin DT, Gu G. Improving the global precipitation record: GPCP Version 2.1. *Geophys. Res. Lett.* 2009; 36:L17808.
55. Archibald S, Roy DP. Identifying individual fires from satellite-derived burned area data. *IEEE Int. Geosci. Remote Sens. Symp. Proc.* 2009; 9:160–163.
56. Oom D, Silva PC, Bistinas I, Pereira JMC. Highlighting biome-specific sensitivity of fire size distributions to time-gap parameter using a new algorithm for fire event individuation. *Remote Sens.* 2016; 8:1–15.
57. Hantson S, Pueyo S, Chuvieco E. Global fire size distribution is driven by human impact and climate. *Glob. Ecol. Biogeogr.* 2015; 24:77–86.
58. Hansen MC, et al. Towards an operational MODIS continuous field of percent tree cover algorithm: Examples using AVHRR and MODIS data. *Remote Sens. Environ.* 2002; 83:303–319.
59. Hantson S, et al. The status and challenge of global fire modelling. *Biogeosciences.* 2016; 13:3359–3375.
60. Li F, Zeng XD, Levis S. A process-based fire parameterization of intermediate complexity in a dynamic global vegetation model. *Biogeosciences.* 2012; 9:2761–2780.
61. Li F, Levis S, Ward DS. Quantifying the role of fire in the Earth system - Part 1: Improved global fire modeling in the Community Earth System Model (CESM1). *Biogeosciences.* 2013; 10:2293–2314.
62. Knorr W, Jiang L, Arneth A. Climate, CO₂ and human population impacts on global wildfire emissions. *Biogeosciences.* 2016; 13:267–282.
63. Smith B, et al. Implications of incorporating N cycling and N limitations on primary production in an individual-based dynamic vegetation model. *Biogeosciences.* 2014; 11:2027–2054.
64. Lehsten V, et al. Estimating carbon emissions from African wildfires. *Biogeosciences.* 2009; 6:349–360.
65. Yue C, et al. Modelling the role of fires in the terrestrial carbon balance by incorporating SPITFIRE into the global vegetation model ORCHIDEE - Part 1: Simulating historical global burned area and fire regimes. *Geosci. Model Dev.* 2014; 7:2747–2767.
66. Yue C, Ciais P, Cadule P, Thonicke K, Van Leeuwen TT. Modelling the role of fires in the terrestrial carbon balance by incorporating SPITFIRE into the global vegetation model ORCHIDEE - Part 2: Carbon emissions and the role of fires in the global carbon balance. *Geosci. Model Dev.* 2015; 8:1321–1338.
67. Lasslop G, Thonicke K, Kloster S. SPITFIRE within the MPI Earth system model: Model development and evaluation. *J. Adv. Model. Earth Syst.* 2014; 6:740–755.
68. Mangeon S, et al. INFERNO: A fire and emissions scheme for the UK Met Office’s Unified Model. *Geosci. Model Dev.* 2016; 9:2685–2700.
69. Arora VK, Boer GJ. Fire as an interactive component of dynamic vegetation models. *J. Geophys. Res.* 2005; 110:G02008.
70. Melton JR, Arora VK. Competition between plant functional types in the Canadian Terrestrial Ecosystem Model (CTEM) v. 2.0. *Geosci. Model Dev.* 2016; 9:323–361.
71. Bachelet D, Ferschweiler K, Sheehan TJ, Sleeter BM, Zhu Z. Projected carbon stocks in the conterminous USA with land use and variable fire regimes. *Glob. Chang. Biol.* 2015; 21:4548–4560. [PubMed: 26207729]
72. Bhaduri B, nad Phillip Coleman EB, Dobson J. LandScan: Locating people is what matters. *Geoinformatics.* 2002; 5:34–37.
73. Dobson JE, Bright EA, Coleman PR, Durfee RC, Worley BA. LandScan: a global population database for estimating populations at risk. *Photogramm Eng Rem Sens.* 2000; 66:849–857.
74. Robinson TP, Franceschini G, Wint W. The Food and Agriculture Organization’s gridded livestock of the world. *Vet. Ital.* 2007; 43:745–751. [PubMed: 20422554]
75. Jahnke HE. Livestock production systems and livestock development in tropical Africa. *Kieler Wissenschaftsverlag Vauk, Kiel, Germany.* 1982; doi: 10.2307/1240913

76. Friedl MA, et al. Global land cover mapping from MODIS: algorithms and early results. *Remote Sens. Environ.* 2002; 83:287–302.
77. Food and Agriculture Organization Statistics division, FAO 2016 (available at <http://faostat3.fao.org>).
78. Pivello VR. The use of fire in the cerrado and Amazonian rainforests of Brazil: Past and present. *Fire Ecol.* 2011; 7:24–39.
79. Hardin G. The tragedy of the commons. *Science.* 1968; 162:1243–1248.
80. Owe M, de Jeu RAM, Holmes T. Multisensor historical climatology of satellite-derived global land surface moisture. *J. Geophys. Res. Earth Surf.* 2008; 113:F01002.
81. Le Page Y, Oom D, Silva JMN, Jönsson P, Pereira JMC. Seasonality of vegetation fires as modified by human action: observing the deviation from eco-climatic fire regimes. *Glob. Ecol. Biogeogr.* 2010; 19:575–588.
82. Lu H, Raupach MR, McVicar TR, Barrett DJ. Decomposition of vegetation cover into woody and herbaceous components using AVHRR NDVI time series. *Remote Sens. Environ.* 2003; 86:1–18.
83. Potter CS, et al. Terrestrial ecosystem production: A process model based on global satellite and surface data. *Global Biogeochem. Cycles.* 1993; 7:811–841.
84. Kahn RA, et al. Multiangle Imaging SpectroRadiometer global aerosol product assessment by comparison with the Aerosol Robotic Network. *J. Geophys. Res. Atmos.* 2010; 115:D23209.
85. Deeter MN, et al. The MOPITT Version 6 product: Algorithm enhancements and validation. *Atmos. Meas. Tech.* 2014; 7:3623–3632.
86. Chen Y, Morton DC, Andela N, Giglio L, Randerson JT. How much global burned area can be forecast on seasonal time scales using sea surface temperatures? *Environ. Res. Lett.* 2016; 11:45001.
87. Field RD, et al. Indonesian fire activity and smoke pollution in 2015 show persistent nonlinear sensitivity to El Niño-induced drought. *Proc. Natl. Acad. Sci.* 2016; 113:9204–9209. [PubMed: 27482096]
88. van der Werf GR, et al. Climate regulation of fire emissions and deforestation in equatorial Asia. *Proc. Natl. Acad. Sci.* 2008; 105:20350–20355. [PubMed: 19075224]
89. Klein Goldewijk K, Beusen A, Van Dreht G, De Vos M. The HYDE 3.1 spatially explicit database of human-induced global land-use change over the past 12,000 years. *Glob. Ecol. Biogeogr.* 2011; 20:73–86.
90. Hurtt GC, et al. Harmonization of land-use scenarios for the period 1500–2100: 600 years of global gridded annual land-use transitions, wood harvest, and resulting secondary lands. *Clim. Change.* 2011; 109:117–161.

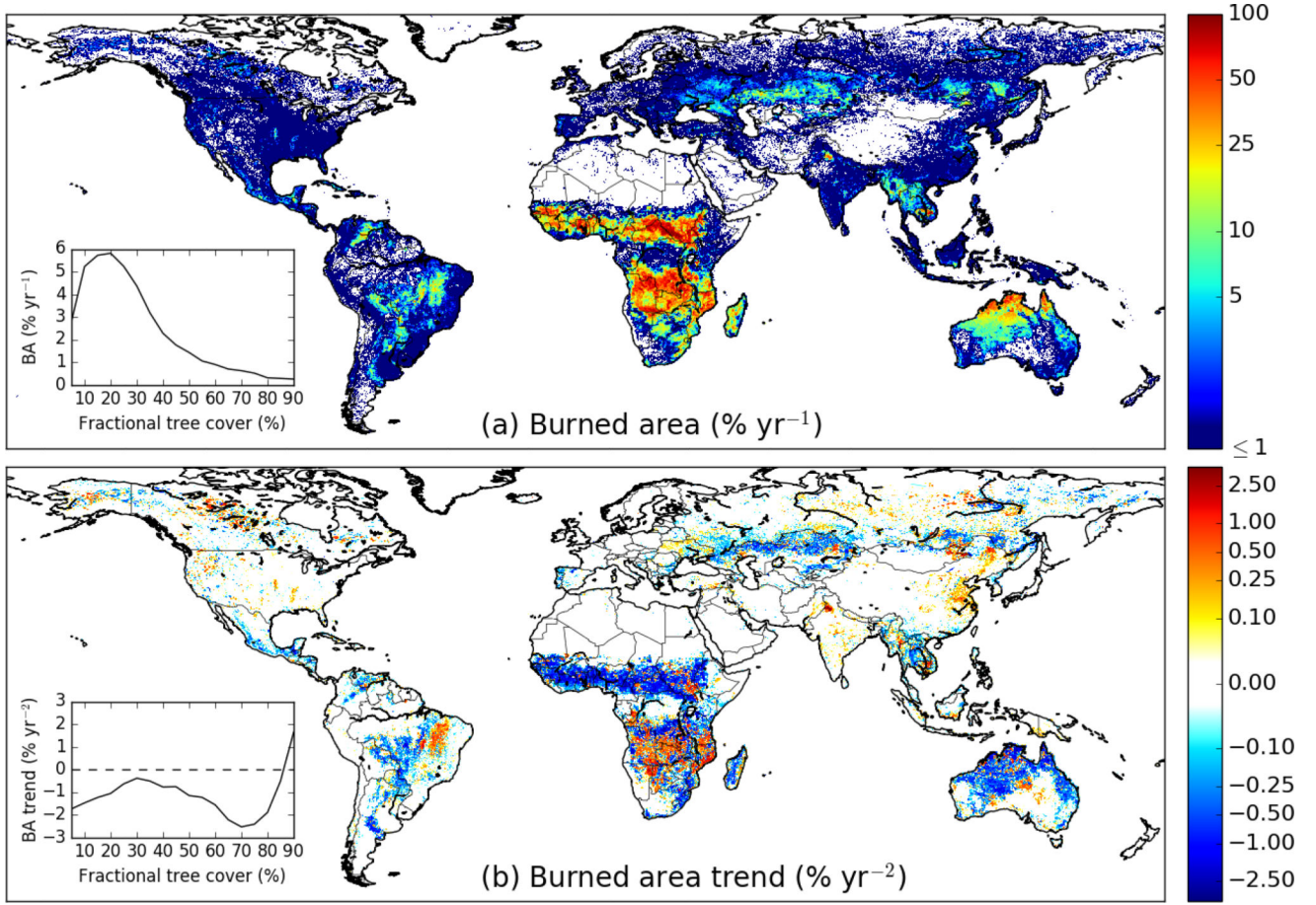


Fig. 1. Satellite observations of (a) mean annual burned area and (b) trends in burned area (GFED4s, 1998 - 2015) show a decline of fire activity across the world's tropical and temperate grassland ecosystems and land use frontiers in the Americas and Southeast Asia. Line plots (inset) indicate global burned area and trend distributions by fractional tree cover (28).

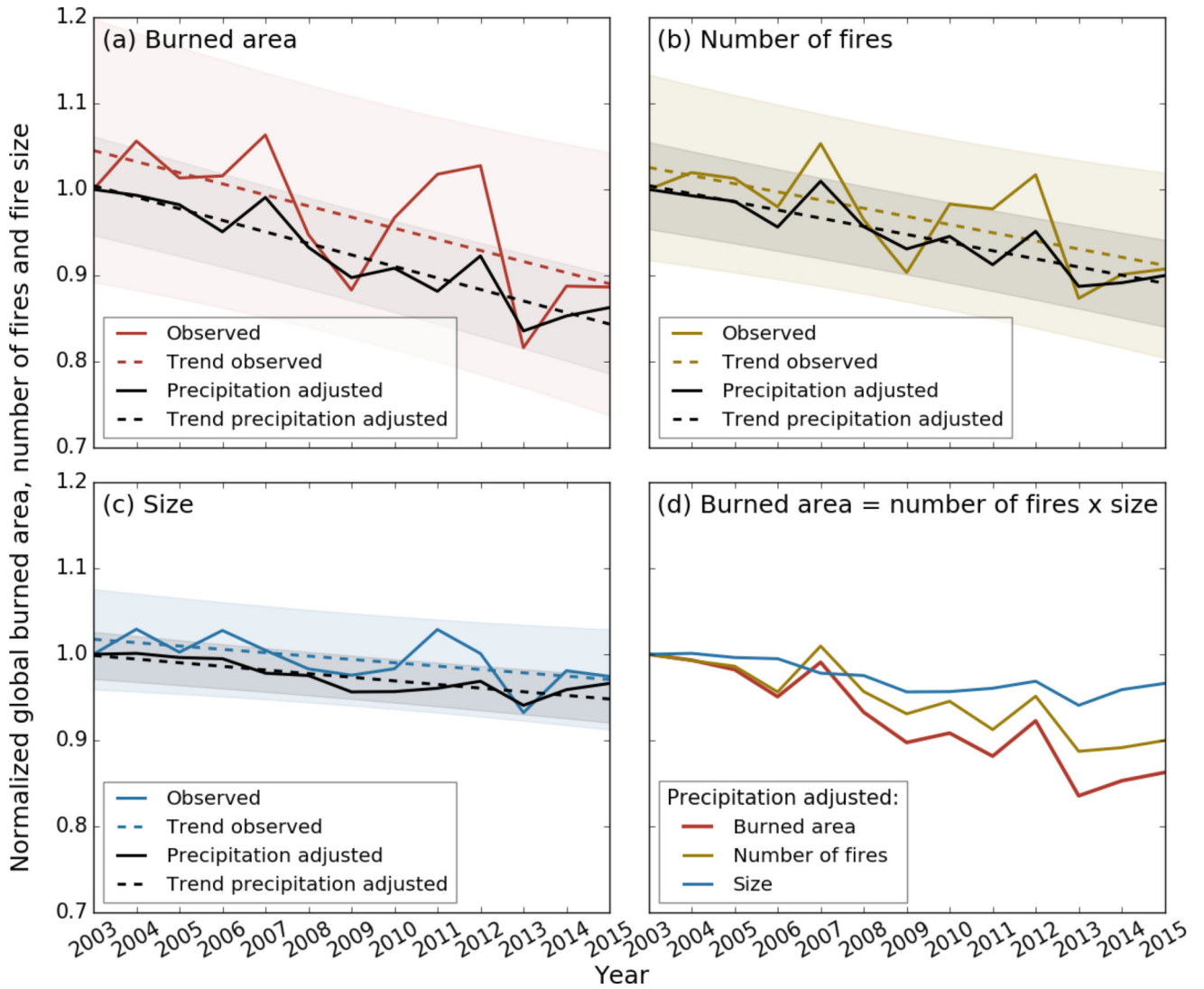


Fig. 2. A decrease in the number of fires was the primary driver of the global decline in burned area (MCD64A1). Normalized variation (2003 = 1) and linear trends in (a) burned area, (b) number of fires, and (c) mean fire size. Shading denotes 95% prediction intervals. Adjusting for precipitation-driven trends in burned area (28) isolated residual trends associated with other factors, including human activity. Panel (d) summarizes trends in global burned area, calculated as the product of the number and size of fires, after adjusting for the influence of precipitation. Regional trends in fire number and fire size are provided in Table 1, S1 and Fig. S7.

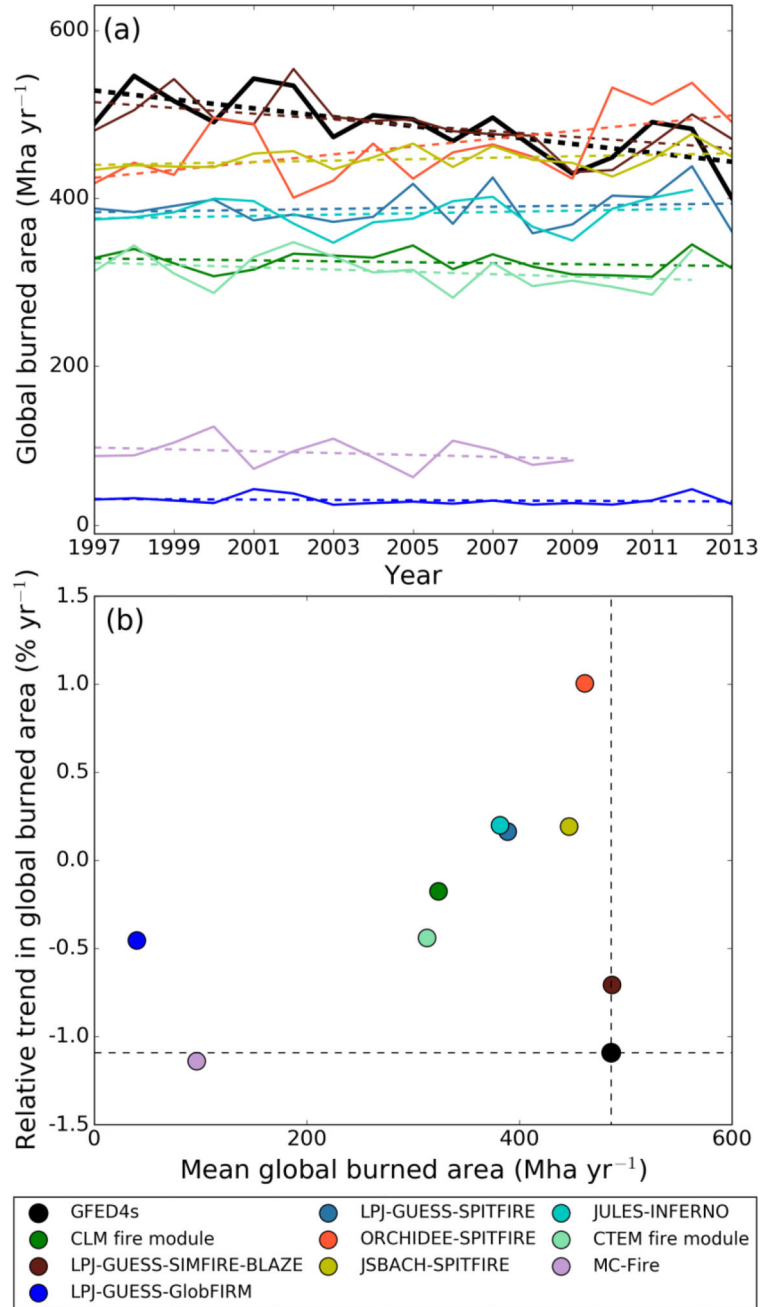


Fig. 3. Comparison of burned area trends from the satellite observations (GFED4s) and prognostic fire models from FireMIP. (a) Time series of global burned area. (b) A comparison of global mean annual burned area versus the relative trend in global mean burned area from the observations and models. GFED4s observations are shown in black and FireMIP models with different colors. FireMIP model estimates were available from 1997 – 2013 for six models, from 1997 – 2012 for the CTEM fire module and JULES-INFERN0, and from 1997 – 2009 for MC-Fire. The FireMIP models are described in more detail in the Supporting Online Material and by *Rabin et al.* (28, 34, Table S3 and S4, Fig. S8).

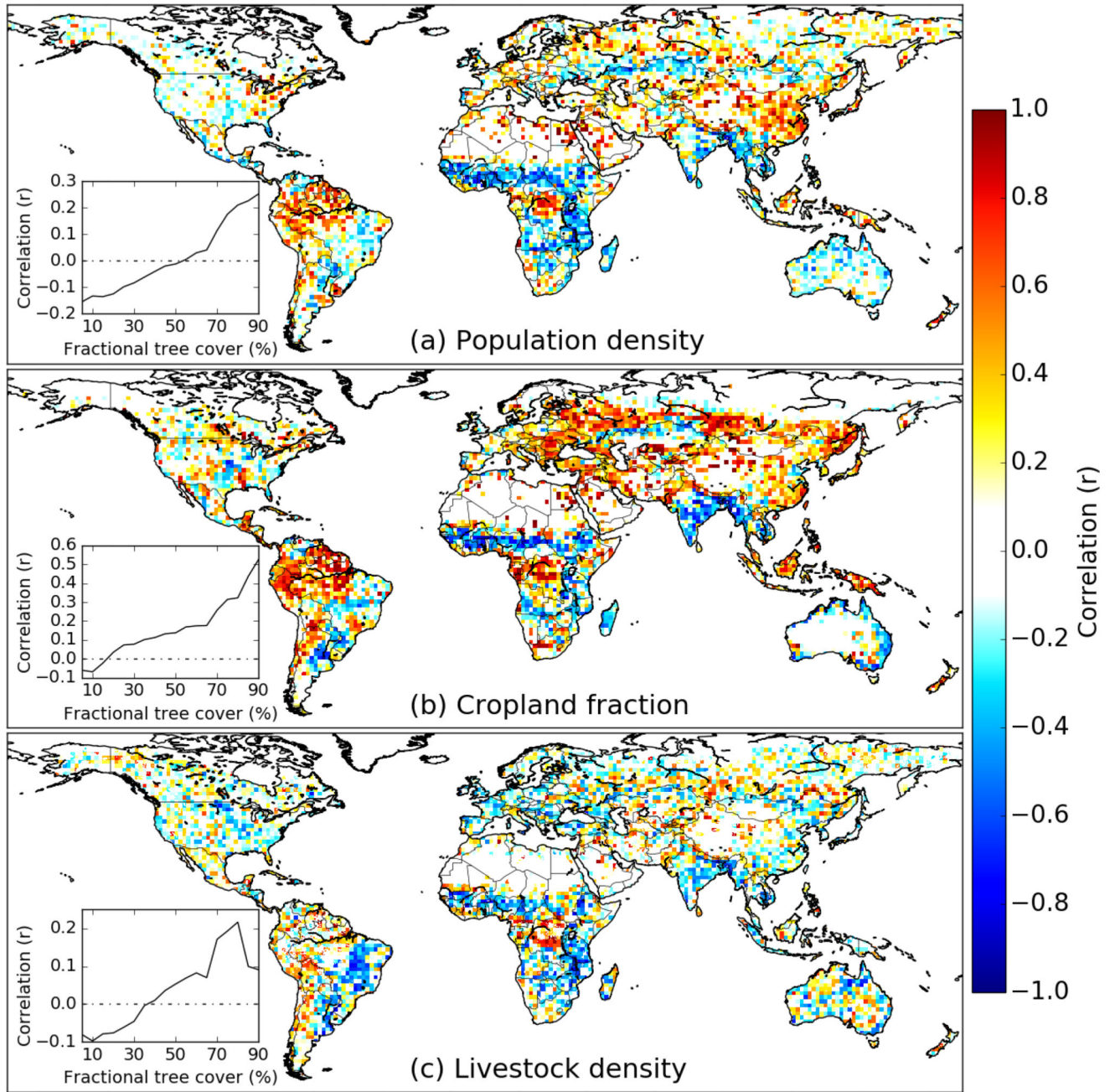


Fig. 4. Maps of the spatial correlation between burned area and (a) population density per km², (b) fractional cropland area, and (c) livestock density per km². Map panels indicate the spatial correlation between burned area (GFED4s) and human land use for the 36 0.25° pixels within each 1.5° grid cell. Line plots (inset) show the mean correlation as a function of fractional tree cover (28).

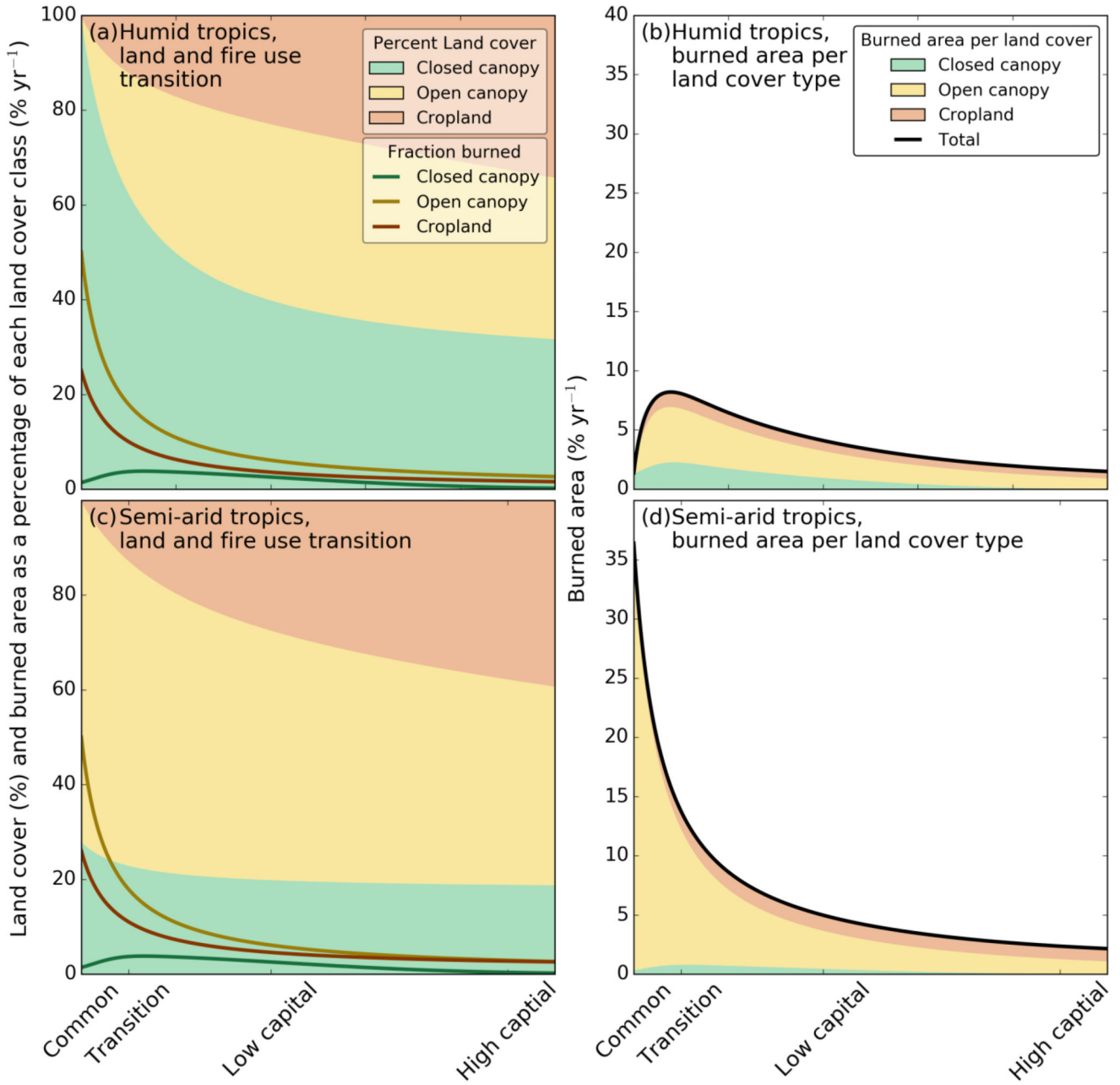


Fig. 5. Conceptual model showing changes in fire use along the continuum from common land ownership to highly capitalized agricultural management on private lands. In humid tropical regions (a,b; precipitation $> 1200 \text{ mm yr}^{-1}$), deforestation fires for agricultural expansion (a) lead to peak burned area during an early land use transition phase to more settled land uses (b). In the semi-arid tropics (c,d; precipitation $500\text{--}1200 \text{ mm yr}^{-1}$), burned area is highest under common land ownership (d), as intact savanna and grazing lands allow for the spread of large fires. Conversion of savanna and grassland systems for more permanent agriculture drives a non-linear decline in burned area from landscape fragmentation and changing fire use for agricultural management. The conceptual model is based on the spatial distribution

of burned area, land use, population, and GDP (28, Fig. S12 and S13). Similar patterns are observed across all continents, but absolute burned area differs as a function of culture, climate, and vegetation.

Table 1

Relative trends in burned area, number of fires, and mean fire size for different regions of the world. Trends are shown for different time periods, as indicated, to directly compare burned area estimates from different sources. All trends were calculated using fire season estimates of burned area, with exception of the FireMIP data, which were produced per calendar year (28).

Fire product	Time period	Full or residual ¹	Trend (% yr ⁻¹) with 95% confidence limits						
			World	North America	South America	Eurasia ²	Southeast Asia	Africa	Australia
Burned area (GFED4s)	1998–2015	Full							
		PA							
Burned area (GFED4s) during the MODIS era	2003–2015	Full							
		PA							
Burned area from 500m MODIS MCD64A1	2003–2015	Full							
		PA							
Fire number	2003–2015	Full							
		PA							
Fire size	2003–2015	Full							
		PA							
Burned area predicted by FireMIP ³	1997–2013	Full							
		PA							

Colors indicate increases (red) and decreases (blue) in burned area for each region and time period; significant trends are denoted by asterisks (* p<0.1, ** p<0.05, and *** p<0.01).

¹ Residual time series, after adjusting for the influence of precipitation variability (PA), were estimated using the approach described in the Supplementary Materials.

² Eurasia excludes regions in Southeast Asia.

³ In this instance, numbers between parentheses are the standard deviation of the trend averaged across the different FireMIP models (n=9).